Modeling the Monte Carlo simulation of associating fluids

Donald P. Visco, Jr. and David A. Kofke
Department of Chemical Engineering, State University of New York at Buffalo, Buffalo, New York 14260

(Received 9 October 1998; accepted 18 December 1998)

We model the Monte Carlo simulation of a simple associating system to understand and quantify the ability of the simulation to provide measurements of the energy and heat capacity. The simulation is examined for its convergence to the equilibrium degree of association, and separately for the precision of its measurements. The molecular model used for the study was proposed by van Roij; it is very simple, and allows the formation of only chain-like association structures while exhibiting only association and no repulsion or dispersion interactions. However, the model captures the essential features that make the simulation of associating systems difficult, and it yields to various types of analysis. Unbiased and biased simulation methods are studied. Modeling is facilitated by coarse-graining the system in terms of the total number of association bonds. A bond-balance kinetic model is used to examine the convergence behavior of the simulation. An unexpected finding is that the strength of association is the sole determinant of the rate of convergence, and that the size (volume) of the association sites does not separately impact the convergence rate. The precision of the calculation is quantified via a variance that is obtained from a Markov model of the simulation. We present contours that quantify the precision to be expected in the energy and the heat capacity, from which one can estimate the confidence limits to be expected when simulating a particular system at a given state with a given number of Monte Carlo trials. The results apply rigorously only to the model used in the study, but they should prove useful in gauging the difficulty to be expected in simulating realistic model systems. The biasing Monte Carlo algorithm offers dramatic improvement in both convergence and precision when simulating strongly associating systems, but it is not particularly helpful for weakly associating systems. The analysis also uncovers a finite-size effect that is manifested when measuring the heat capacity in strongly associating systems. © *1999 American Institute of Physics*. [S0021-9606(99)50512-6]

I. INTRODUCTION

Over the past decade Monte Carlo simulation has advanced rapidly through new ensemble construction and novel simulation techniques. These advances, in conjunction with increased computing power, have allowed researchers to explore more complex fluids. Associating fluids are one such class of systems which has received increasing attention over the past decade. Powerful theories have been developed to treat these associating fluids, and molecular simulations of these systems have been conducted to support the theory development. However, only recently have specialized simulation methods emerged which are formulated to overcome the difficulties involved in simulating associating systems.

Association typically occurs when a highly electronegative species that is chemically bonded to a hydrogen atom removes electron density from the hydrogen atom. This localized ''positive charge'' allows for another highly electronegative specie (either on the same or different molecule) to form a relatively strong but highly constrained bond with the hydrogen atom.[1] Accordingly, a potential energy surface which describes the interactions between two species that associate will exhibit deep but narrow wells representing this energetically favorable situation.

In the simplest models of associating fluids, the association interaction is treated as a square-well bonding site. The square-well model possesses the two basic features of association, namely a well depth and width which can be set via judicious choice of parameters. More realistic models of associating systems usually attach an electrostatic contribution (e.g., Coulombic point charges) to a simple model potential, usually the Lennard-Jones (LJ) model.[2,3] In bonded configurations the attractive part of the LJ potential is usually insignificant relative to the Coulombic interactions, but the LJ attraction is still very important; without it the system will exhibit no vapor–liquid phase equilibria, even if association is very strong.[4] The repulsive part of the LJ potential prevents the molecules from getting too close, and forming unrealistically strong bonds via the Coulombic sites.[5]

The open literature is filled with simulations of model potentials that account for association.[6–15] Many of these works have been done as a result of or in conjunction with the verification of the Statistical Associating Fluid Theory (SAFT).[16] Since SAFT is based on a simplistic division of the Helmholtz free energy into specific parts accounting for different types of interaction, one can verify the validity of some parts of the theory for certain conditions through the use of Monte Carlo (MC) simulation.

Molecular simulation is often performed using the Metropolis Monte Carlo method, which is designed to sample configuration space along the Boltzmann distribution of the ensemble of interest. In theory, the Metropolis method will work for all potential models provided enough configurations are realized. In practice, however, the simulation of complex

systems is likely to encounter bottlenecks or traps in configuration space. It is good to find these traps, because they are an important part of the physics of the system, but it is not good to be trapped by them. The result of being trapped is poor exploration of the other parts of configuration space during a *reasonable* simulation length. In associating systems the traps are the bonded configurations. Bonded configurations form a very small part of all of configuration space, but they, nevertheless, have a very large Boltzmann weighting because of their favorable energy. Thus the simulations of these types of models may suffer from two distinct yet complimentary problems; first, the simulation may have trouble locating these important configurations, and second, once they are there they may take an exceedingly long time to leave.

Various steps may be taken to alleviate the sampling problems of associating systems. The first recognizes that the length scale of hydrogen-bonding interactions is different than other types of interactions, and accounts for this explicitly by allowing for two types of displacement moves.[8] The advantage of this approach is that it is very simple, and that it facilitates exploration of configurations once association has taken place; otherwise if all displacements, bound and unbound, are governed by the same (large) step size, bound molecules would not likely experience any successful moves until they become unbound. This dual-step mechanism still does not address the need for potential wells to be entered and left with a high frequency. The solution to this problem is the application of biased trial moves to directly take molecules into and out each others' bonding regions during the course of the simulation; the bias so introduced in the trial step is removed in the acceptance step. Obviously the advantage of this approach is that it ensures the exploration of the salient parts of configuration space in a reasonable simulation length. Another approach relies on the configurational-bias method, which has proven very successful in simulating macromolecules, particularly chains.[17] However, in its current form, this method does not allow for bonding and unbonding moves and, thus, does not address the sampling problems of associating systems.

Recently two groups have proposed biasing algorithms specifically for associating systems. The association biased Monte Carlo (ABMC) method of Busch *et al*. was used in the simulation of a binary, symmetric, associating LJ fluid with single[6] and multiple[18] sites on each particle. The algorithm is rather complex, involving two particle displacements per biased trial move, with the detailed identification of all bonding regions within the second displacement sphere. However, it does not invoke any special features of the bonding potential to simplify the algorithm, so it is rigorously correct (assuming one is capable of programming it correctly). The bond-bias Monte Carlo (BBMC) method was proposed by Tsangaris and de Pablo[7] almost simultaneously with the appearance of ABMC. Tsangaris and de Pablo formulated and used their method to study phase equilibria in LJ particles with strongly associating conical (square-well type) dimerization sites. Their algorithm supplements the Gibbs-ensemble transfer move with a transfer move that is biased toward the formation of a bond. The molecular model excludes the possibility that more than one molecule may be in another's bonding volume. The BBMC approach exploits this feature to yield a much simpler algorithm than ABMC.

Since the biased moves are the ones which guarantee exploration of the deep potential wells but which are in general costly and complicated to implement, it would be useful to have a way to determine *a priori* if at a given thermodynamic state a simulation might benefit from the use of a biasing scheme. The Tsangaris and de Pablo paper describing the BBMC method begins to address this question. They compare normal Gibbs-ensemble results to Gibbs-ensemble results using their biased move for various association strengths and conclude that unbiased simulations will fail for a square-well depth greater than ten times that of the LJ energy parameter.[7] This rule of thumb can be helpful in deciding when to apply a biasing algorithm, but it would be worthwhile to have also a more quantitative and complete characterization of when and how a simulation of an associating system fails.

Thus our aim in this work is to characterize the convergence of MC simulations of associating systems. The convergence behavior of a simulation has two distinct facets. First, there is the question of how long a simulation takes to relax from a nonequilibrium initial configuration; second is the question of how precisely can a simulation provide a given thermodynamic property, i.e., how reproducible is the result? Of course, these questions can be addressed by performing simulations and studying these aspects of their behavior. But since we are interested in identifying those thermodynamic states where simple simulation strategies struggle, we must by definition perform very many and/or very lengthy simulations to obtain an accurate characterization; in fact, there are especially difficult (but relevant) thermodynamic states for which an unbiased simulation could never be equilibrated using present day computers. In such instances it is hopeless to expect the simulation to quantify its own convergence behavior. An alternative is an approach that models the simulation process itself. A good model of the simulation can be studied analytically to yield valid convergence measures, and in much less time than is needed to gain this information from the simulations themselves. This is the approach we use in the present study.

Much of the behavior we aim to understand is manifested in the simulation of very simple molecular models, and by working with simple molecular models we ease the task of modeling simulations of them. In Sec. II we present the molecular model used in this study and review its previously published analytic solution. We also introduce a mesostate approach used to characterize the system. In Sec. III we present a simple kinetic model that describes the convergence of a simulation. In Sec. IV we introduce a biasing algorithm similar to the BBMC algorithm of Tsangaris and de Pablo, but which is suitable for the simulation of bivalent associating fluids; we demonstrate its improved convergence properties via the kinetic model. In Sec. V we present a more detailed approach to modeling the simulation, based on the use of a coarse-grained transition-probability matrix (TPM). This treatment provides information regarding the precision of the simulation averages. In Sec. VI we look at the aver-

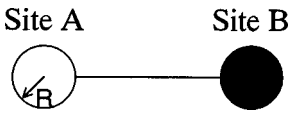

FIG. 1. A cartoon of a molecule in the Ideal Association Model. The radius of both spheres is denoted R. Only when the center of an $A(B)$ site is inside a $B(A)$ site on another molecule does bonding occur.

ages and variances obtained from the TPM for the energy and heat capacity of the model over a large range of states. Section VII provides concluding remarks.

II. IDEAL ASSOCIATION MODEL

A. Molecular model

A very simple molecular model that exhibits only association is realized by placing square-well sites on otherwise ideal particles. A diagram of such a model is presented in Fig. 1. Each molecule forms a heteronuclear diatomic with spherical sites A and B each of radius R. In the figure the sites are set apart from each other by some distance, but this does not affect the thermodynamic properties in any way. When the *center* of site A (or B) on molecule i is within site B (or A) on molecule j, there is an energy of interaction equal to $-\epsilon$ given as

$$U_{ij}=\begin{cases}-\epsilon & R_{Ai,Bj}<R \\ 0 & R_{Ai,Bj}\geqslant R\end{cases}, \tag{1}$$

where $R_{Ai,Bj}$ is the distance between the center of site A on molecule i and the center of site B on molecule j. This is the only interaction that the molecules have with one another. We call this the Ideal Association Model (IAM), and it was introduced and studied by van Roij[19,20] in his work on chain association and liquid condensation. By definition this model disallows the formation of any species other than straight chains, and in particular rings and branched structures are excluded. Additionally, the analysis of this model by van Roij includes an implicit assumption that the bonding volume of a molecule is small relative to the system volume per molecule.

Van Roij has presented the IAM canonical-ensemble partition function and free energy[20]

$$Z_{id}(\{N_i\},V,T)=\prod_i \frac{V^{N_i}}{N_i!\,\nu_i^{N_i}}, \tag{2}$$

$$\beta F_{id}(\{N_i\},V,T)=\sum_i N_i\left(\log\left(\frac{N_i\nu_i}{V}\right)-1\right), \tag{3}$$

where V is the volume, T is the temperature and N_i is the number of molecules of specie i. The term ν_i is the thermal volume of an i-mer.

Through application of the law of mass action and the chemical equilibrium condition,[20,21] one can show that the distribution of chains at a given state is

$$N_i=\frac{N}{A}\left(1-\left(\frac{1}{2A}\right)(H-1)\right)^i =\frac{N}{A}Y^i \tag{4}$$

where $H=(4A+1)^{1/2}$, $A=\rho V_{\text{eff}}\exp(\beta\epsilon)$, and V_{eff} is the bonding volume for two molecules, $V_{\text{eff}}=\frac{4}{3}\pi R^3$; the (apparent) number density $\rho=N/V$. The quantity Y is defined from Eq. (4). It is notable that in this simple model the oligomer chain distribution depends on temperature and density only through their presence in the group A. The association parameter A characterizes the degree to which association is relevant: larger values of A correspond to greater degrees of association, an increased population of larger oligomers, and greater deviation from (apparent) ideal-gas behavior.[20] Given the distribution of oligomers at equilibrium, it is a simple matter to determine the equilibrium thermodynamic properties. An oligomer of length i has an energy $-\epsilon(i-1)$, so the total energy per molecule u is

$$u=-\frac{\epsilon}{N}\sum_i N_i(i-1). \tag{5}$$

Further, the heat capacity is obtained via differentiation of u with respect to temperature which yields

$$C_v/NK_b=\frac{\beta^2\epsilon^2}{A}\sum_i (i-1)\left(iY^{i-1}\left(\frac{H-1}{2A}-\frac{1}{H}\right)-Y^i\right), \tag{6}$$

with K_b as Boltzmann's constant.

The equation of state is that of an ideal gas of oligomers

$$\beta P=\frac{\rho}{\chi}, \tag{7}$$

where χ is the association number, defined as $\chi=N/\Sigma_i N_i$.

We work with this model because it contains the fewest number of parameters needed to characterize an associating system, it is analytically solvable, and it provides for an unambiguous definition of what constitutes an association bond.

B. Mesostates

The basic approach we use to model the Monte Carlo simulation of associating systems consists of a coarse-graining of the detailed molecular configurations into a set of ''mesostates'' characterized only by the total number of association bonds (called here a bond number), denoted S. All possible configurations and oligomer distributions consistent with a particular bonding number are grouped into the same mesostate. We then concern ourselves with how well the simulation moves from one of these mesostates to another. Information lost during the coarse-graining process is incorporated in the approximate description of this transition process.

We collect here some basic results for the IAM as a function of the bond number S. The number of monomers to be expected in a system of given N and S is an important quantity in modeling the simulation. For this model all states

of a given S have the same energy, so the monomer fraction can be deduced through a simple probabilistic argument. We consider picking a molecule at random in the system, and ask what is the likelihood that both its A and its B site are unbonded. At a given (N,S) state there are S molecules that have their A site bonded. Thus the probability that a molecule's A site is bonded is given as $P(A)=S/N$. Likewise, the probability that a molecule's A site is *not* bonded is $P(\bar{A})=1-(S/N)$. Once a molecule has its A site bonded, the probability that its B site is bonded is $P(B|A)=(S-1)/(N-1)$. Finally, the probability that a molecule's B site is bonded given that its A site is *not* bonded is $P(B|\bar{A})=S/(N-1)$. From these probabilities, we can determine the probability of a monomer as $P(\bar{A}\cap\bar{B})$

$$P(\bar{A}\cap\bar{B})=P(\bar{B}|\bar{A})P(\bar{A}) \tag{8}$$

$$=(1-P(B|\bar{A}))P(\bar{A}) \tag{9}$$

$$=\left(1-\frac{S}{N-1}\right)\left(1-\frac{S}{N}\right). \tag{10}$$

Thus the number of monomers at a given N and S is

$$N_1=N-\left(\frac{2N-1}{N-1}\right)S+\left(\frac{1}{N-1}\right)S^2, \tag{11}$$

$$N_1\approx N-2S+\frac{1}{N}S^2, \tag{12}$$

and the probability that a randomly selected molecule is a monomer is

$$P(N_1)\approx\left(1-\frac{S}{N}\right)^2, \tag{13}$$

where we have made a large N approximation.

It is also useful to know the number N_E of segments bonded to exactly one other segment (i.e., the number of segments located at a chain end). This is needed to form the trial probability for going from the $S+1$ to S mesostate. This term is easily derived from N_1, S, and N, via the following argument. If, in addition to N_1 and N_E we define N_M as the number of particles with two bonds (middles), then the total number of bonds in a system satisfies

$$S=\tfrac{1}{2}(N_E+2N_M), \tag{14}$$

where the (1/2) accounts for the double counting. If we consider also the normalization condition

$$N=N_1+N_E+N_M, \tag{15}$$

we can obtain the following relationship for the number of ends and middles at a given N, S, and N_1

$$N_E=2(N-N_1-S), \tag{16}$$

$$N_M=2S-N+N_1. \tag{17}$$

If N_1 is given via the probabilistic argument above, N_E can then be estimated as

$$N_E\approx 2S(N-S)/N. \tag{18}$$

III. KINETIC MODEL OF MC SIMULATION

In the present section we describe the convergence of the simulation via a simple kinetic bond-balance model, called here ''kinetic model'' for short. We characterize the convergence via the bond number S, which we attempt to determine as a function of simulation length, assuming the initial configuration has no bonded configurations. Our aim it to identify a simple measure through which we can gauge the length of simulation needed to bring the system close to equilibrium. This approach does not provide information about the precision we might expect in the simulation averages; for that we rely on a Markov-process modeling approach described in Sec. V.

The kinetic model treats the formation and destruction of bonds as a reaction that increases or decreases the total number of bonds S. In particular we write

$$\frac{dS}{dt}=k_f-k_r. \tag{19}$$

Here t is a ''time scale'' which is proportional to the simulation length (the time scale being simulation cycles), k_f is the rate of bond formation, and k_r is the corresponding quantity for bond breakage. These quantities are functions of the bond number S. In essence this approach is just a balance on the number of bonds in the system where the time derivative of S is an accumulation term.

The rates of bond breakage and formation depend on details of the simulation algorithm. We consider in this section a simulation performed using the standard Monte Carlo method, while in the next we apply this model to a bond-bias simulation algorithm. During an unbiased Monte Carlo simulation in the NVT ensemble, thermal equilibrium is achieved through the use of particle displacements and rotations. A particle is chosen at random and moved to a random position (or rotated to a random orientation). For simplicity, we assume that only three mutually exclusive outcomes can occur as a result of this move: (1) the particle begins as a monomer (i.e., it has no association bonds with other molecules) but bonds with another molecule as a result of the movement; (2) the particle begins as an end of a chain and becomes a monomer as a result of the movement; (3) the move causes the formation or destruction of no bonds. In principle, other outcomes are possible but are much less likely than the ones we include, at least in situations of interest to this study. For example, it is possible to have the destruction or formation of two bonds simultaneously (a molecule is removed from the middle of a chain, or is inserted in a way that bridges the ends of two separate chains); also it is possible for a chain end to be moved such that it forms a bond to another chain end. Ignoring the latter is not as safe as the neglect of double bond-change outcomes, but their inclusion complicates the model to a degree disproportionate to their importance.

The forward rate k_f is determined by outcome (1) above. The formation of a bond involves the following events, which occur with the probabilities indicated in brackets: (a) a monomer is selected $[N_1/N]$; (b) the monomer trial displacement causes it to be put into the bonding volume of an unsaturated segment, either another monomer or a chain end

$[(2N_1+N_E)V_{\text{eff}}/V]$; (c) the trial move is accepted $[\min(1,\omega)]$. Here $\omega=\exp(\beta\epsilon)$ and since we are concerned only with the states where $\epsilon>0$, the acceptance probability is unity. Thus the forward rate is given as the product of these probabilities

$$k_f=\frac{N_1}{N}\left(\frac{N_E+2N_1}{N}\right)\rho V_{\text{eff}}. \tag{20}$$

The reverse rate k_r depends on outcome (2). Bond destruction involves the following events: (a) a chain end is selected $[N_E/N]$; (b) it is placed as a monomer $[(V-NV_{\text{eff}})/V\approx 1]$; (c) the trial move is accepted $[\min(1,1/\omega)]$. The reverse rate is then

$$k_r=\frac{N_E}{N}e^{-\beta\epsilon}. \tag{21}$$

This model for the breakage move assumes the chain end is placed randomly within the entire simulation volume. This may be practically the case in an actual simulation if the displacement step size is sufficiently large; a smaller step size would diminish this bond-breakage rate.

We can now apply the relations for $N_1(S)$ and $N_E(S)$ developed in the previous section to assemble a complete kinetic formula for the evolution of the bond number S. It is convenient to write this in terms of the intensive variable $s\equiv S/N$:

$$N\frac{ds}{dt}=2(1-s)^3\rho V_{\text{eff}}-2s(1-s)e^{-\beta\epsilon}. \tag{22}$$

The variables may be separated and integrated with t given as a function of s

$$\begin{aligned} t/N=&\frac{1}{4\exp(-\beta\epsilon)}\ln((s-1)^2)\\ &-\frac{1}{4\exp(-\beta\epsilon)}\ln|As^2-(2A+1)s+A|\\ &-\frac{1}{4\exp(-\beta\epsilon)H}\ln\left|\left(\frac{1+\frac{D}{H}}{1-\frac{D}{H}}\right)\right|, \end{aligned} \tag{23}$$

where $D=-2A+2As-1$, and H defined from Eq. (4).

We can use Eq. (22) to determine the steady-state value for s which is

$$s(t\to\infty)=1+\frac{1-H}{2A}. \tag{24}$$

In comparison, we can determine the equilibrium value for s from the IAM through use of Eqs. (4) and (5):

$$s=\sum_{i=1}^{\infty}N_i(i-1), \tag{25}$$

$$s=\frac{(2A-H+1)^2}{A(H-1)^2}, \tag{26}$$

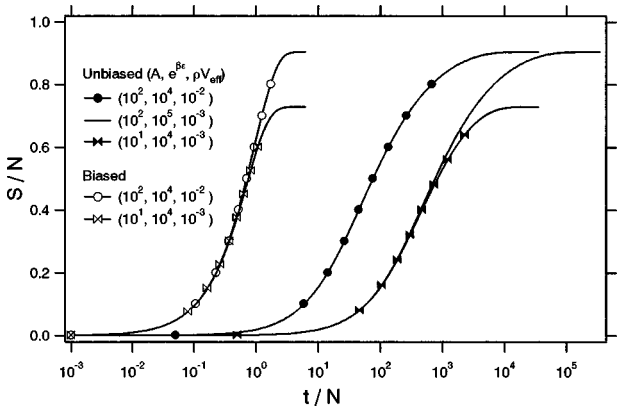

FIG. 2. The bond number per molecule as a function of simulation cycle (one cycle=one attempted move for each molecule). The state is listed as $(A,\exp(\beta\epsilon),\rho V_{\text{eff}})$. Each curve ends at the point where the transient value for S/N is within $10^{-4}\%$ of the steady-state value. For the unbiased and biased algorithms, equal values for A result in the same steady-state value for the bond number. For the unbiased algorithm, two states with equal $\exp(\beta\epsilon)$ but different values of A will converge to different steady-state values for the bond number but reach steady-state at the same time. The biased algorithm shows the same convergence rate regardless of the value for $\exp(\beta\epsilon)$. We do not show the state $(10^2,10^5,10^{-3})$ for the biased algorithm as it follows the same curve for the state $(10^2,10^4,10^{-2})$.

which will simplify to the steady-state value obtained from the kinetic model analysis and providing some validation of the kinetic approach applied here.

The decay rate is of primary interest in this analysis. A careful look at the coefficients of the logarithms on the right-hand side of Eq. (23) indicates that the time constant for the decay of the s to its equilibrium value goes as $\exp(\beta\epsilon)$. The decay time depends only on the bonding strength, and not on the bonding volume. Thus if two states are defined by the same value of A but differ in $\exp(\beta\epsilon)$ (and thus in ρV_{eff}), they will have the same steady-state (equilibrium) energy but different convergence rates. Likewise, two states with the same value for $\exp(\beta\epsilon)$ but different values for A (and thus again different values of ρV_{eff}) will converge at the same rate, but to different energies. This is shown in Fig. 2, where we present s as a function of t according to Eq. (23). We have verified this result by Monte Carlo simulation of the model system.

IV. BIASING ALGORITHM

We describe in this section a simple biasing algorithm that can help offset the sampling difficulties found in the type of system presently studied. The basic approach in the method involves forcing trial moves in which a monomer is preferentially added to or removed from the end of a chain. We call the approach MASA, for the Monomer Addition–Subtraction Algorithm. It is very similar to the BBMC method of Tsangaris and de Pablo, but it is suitable for simulating chain-forming aggregates. It has already been used in a modified form to aid in the MC simulation of hydrogen fluoride vapor.[22]

MASA trial moves are mixed in with standard MC trial moves (particle displacement, rotation, etc.) with some predetermined frequency. In each MASA move, an oligomer

TABLE I. Determining the acceptance criteria for the forward and reverse moves of the MASA. Here, $\omega^*=(N_C/N)\rho V_{\text{eff}}\exp(\beta\epsilon)$, where N_C is the total number of oligomers.

	$i\to j$	$j\to i$
Choose a molecule	$\frac{1}{N_C}$	$\frac{1}{N_C-1}$
Choose another molecule	$\frac{1}{N_C-1}$	
Choose an end	$\frac{1}{2}$	$\frac{1}{2}$
Place in bonding ($i\to j$) or nonbonding ($j\to i$) location	$\frac{1}{V_{\text{eff}}}$	$\sim\frac{1}{V}$
Accept move	$\min(1,\omega^*)$	$\min(1,1/\omega^*)$

chain is selected at random. If the chain is a monomer, an addition move is attempted; otherwise the trial attempts to remove a segment from the end of the chosen oligomer. The addition move proceeds as follows. Another oligomer chain (possibly a monomer) is selected at random, and one end of the chain is selected. The monomer is placed at random (position and orientation) such that it is bonded to the selected chain end. In the subtraction move, a segment is selected from either end of the chain. It is then placed at random (position and orientation) with uniform probability in the simulation volume. If the placement finds the segment bonded in any way, such that is not a monomer in its new position, another attempt is made to place it randomly within the volume; this repositioning is repeated until the segment is placed as a monomer. The trial moves are accepted with probabilities given in Table I.

From this information, we can extract convergence information for these biased moves from a kinetic model in the same way as the normal MC moves presented in the previous section. Note that here and in the rest of the work, the term ''biased algorithm'' implies all biased moves and no other type of moves.

As before, we write

$$\frac{dS}{dt}=k_f^*-k_r^*, \tag{27}$$

where the asterisk indicates that these rates are solely for the biased moves. Thus the rates are written as

$$k_f^*=\frac{N_1}{N_C}\min(1,\omega^*), \tag{28}$$

$$k_r^*=\frac{N_C-N_1}{N_C}\min(1,1/\omega^*). \tag{29}$$

Once again, N_C is the number of oligomers at that state and $\omega^*=(N_C/N)A$. An oligomer balance gives the number of oligomers as

$$N_C=N_1+N_E/2, \tag{30}$$

from which we can write

$$\omega^*=(1-s)A. \tag{31}$$

Since ω^* is a function of s, we must derive relationships for t as a function of s considering separately $\omega^*\geqslant 1$ and $\omega^*<1$. For $\omega^*\geqslant 1$,

$$t/N=\frac{-1}{2}\ln(As^2-(2A+1)s+A)+\frac{1}{2H}\ln\left|\left(\frac{1+\frac{D}{H}}{1-\frac{D}{H}}\right)\right|, \tag{32}$$

while for $\omega^*<1$

$$t/N=-\frac{1}{H}\ln\left|\left(\frac{1+\frac{D}{H}}{1-\frac{D}{H}}\right)\right|. \tag{33}$$

These two formulas must be spliced together at the value of s where $\omega^*=1$ (if ω^* goes through this value); this is done by simply translating the time variable of the later time solution.

For large A, the long-time value of ω^* goes as $A^{1/2}>1$ and thus Eq. (32) applies. In this regime also $H\sim A^{1/2}$, so the time constant for the convergence is dominated by the coefficient of the first term on the right-hand side, which is independent of the system parameters. For small A Eq. (33) applies at long times. Here the decay constant depends on H, which is independent of A for small A, and again the convergence rate is independent of the system parameters. Thus we find generally that the convergence rate of the biased simulation does not depend on the state. This outcome is demonstrated in Fig. 2.

Clearly, the biased algorithm, with three to four orders of magnitude improvement in the convergence rate over the unbiased method, demonstrates the efficiency of such a biased approach in simulating associating systems.

V. MARKOV MODEL OF MC SIMULATION

We now consider a model for the simulation in which the transition between the mesostates is described as a Markov process. The Markov model is formulated by constructing a transition-probability matrix (TPM) based on the detailed trial and acceptance probabilities of the bond forming/breaking transitions presented in the previous sections. Having dealt with convergence issues there, we focus the Markov analysis here on the limiting distribution, for which we extract measures of the expected precision of the simulation averages. A complete analysis is possible because the set of coarse-grained states is relatively small; the coarse-graining approach here yields no more than N relevant mesostates.

A. Construction of transition-probability matrix

From the elementary displacement moves we can infer a set of transition probabilities for movement between the mesostates that we have defined. The transition probabilities

that form the elements of the TPM are the same as derived in the kinetic approach of the previous section. Thus for the unbiased algorithm we have

$$\pi_{S,S+1}=k_f\,, \tag{34}$$

$$\pi_{S,S-1}=k_r\,, \tag{35}$$

$$\pi_{S,S}=1-\pi_{S,S+1}-\pi_{S,S-1}\,. \tag{36}$$

We fill the diagonal elements of the TPM by requiring that all the rows sum to unity. Thus the matrix representation of the TPM, which we will call Π is given as:

$$\begin{pmatrix} \pi_{0,0} & \pi_{0,1} & 0 & \cdots & \cdots & \cdots & 0 \\ \pi_{1,0} & \pi_{1,1} & \pi_{1,2} & 0 & \cdots & \cdots & \vdots \\ 0 & \pi_{2,1} & \pi_{2,2} & \pi_{2,3} & 0 & \cdots & \vdots \\ 0 & 0 & \pi_{3,2} & \pi_{3,3} & \pi_{3,4} & \ddots & \vdots \\ \vdots & \cdots & 0 & \ddots & \ddots & \ddots & 0 \\ \vdots & \cdots & \cdots & \ddots & \pi_{N-2,N-3} & \pi_{N-2,N-2} & \pi_{N-2,N-1} \\ 0 & \cdots & \cdots & \cdots & 0 & \pi_{N-1,N-2} & \pi_{N-1,N-1} \end{pmatrix}.$$

The corresponding development for the biased-trial algorithm yields for its elements of the TPM:

$$\pi^*_{S,S+1}=k^*_f\,, \tag{37}$$

$$\pi^*_{S,S-1}=k^*_r\,, \tag{38}$$

$$\pi^*_{S,S}=1-\pi^*_{S,S+1}-\pi^*_{S,S-1}\,. \tag{39}$$

B. Analysis of transition-probability matrix

One can obtain the limiting distribution from the TPM by two methods. Since the limiting distribution must be a solution to the eigenvalue equation $\Pi^\infty\Pi=\Pi^\infty$, then Π^∞ (i.e., multiplication of Π by itself a large number of times) will have all rows equal to the limiting distribution. A more efficient route is found via application of the Perron–Frobenius theorem[23] which allows us to calculate directly the limiting distribution from the eigenvector of the unity eigenvalue of the TPM. We denote this limiting distribution vector, properly normalized, with the symbol **W** (with elements w_i).

The ensemble average of the energy per molecule obtained via this method is given as

$$\langle u\rangle=-\frac{\epsilon}{N}\sum_i\,(i-1)w_i\,. \tag{40}$$

The corresponding formula for the heat capacity is

$$\langle C_v\rangle/NK_b=\beta^2\epsilon^2\sum_i\,w_i(i-1)^2 - \beta^2\epsilon^2\left(\sum_i\,w_i(i-1)\right)^2. \tag{41}$$

The precision of the averages for the thermodynamic properties can be obtained from knowledge of occupancy statistics derived from the TPM. In particular, we can obtain statistics for the occupancy variances and covariances via the following formula, written for the limiting case of very large sample size M[24,25]

$$M\langle\gamma_i\gamma_j\rangle=\phi_i\phi_j+\phi_i f_{ij}+\phi_j f_{ji}-\delta_{ij}\phi_i\,. \tag{42}$$

Here $\langle\gamma_i\gamma_j\rangle$ are the occupancy variance statistics. These quantities are interpreted as follows. One performs many (essentially infinite) simulations, each of length M (which is large enough for each simulation to reach its limiting distribution). In a given simulation, the occupancy of a state j (the fraction of the time the system has a bond number S_j) will differ from the expected value, and we denote this difference γ_j. The variance in γ_j and its covariance with the occupation deviation in another state i are the quantities given by this formula. The variances in the thermodynamic averages are obtained from these statistics using standard propagation-of-error formulas, as detailed below.

In Eq. (42), ϕ_j is the limiting probability that state j will be occupied and $\delta_{i,j}$ is the Kronecker delta function. The term f_{ij} above are the elements of the matrix

$$\mathbf{F}=(\mathbf{I}-\Pi+\Pi^\infty)^{-1}-\Pi^\infty. \tag{43}$$

Propagation of error is applied to predict the fractional variance in the average bond number $\langle S\rangle$

$$M\sigma_S^2=\frac{1}{\langle S\rangle^2}\sum_i\,\sum_j\,M\langle\gamma_i\gamma_j\rangle S_iS_j\,. \tag{44}$$

The fractional variance in the energy is identical to this. Propagation of error for the fractional heat-capacity variance leads to

$$M\sigma_{Cv}^2=\frac{1}{\langle C_v\rangle^2}\sum_i\,\sum_j\,M\langle\gamma_i\gamma_j\rangle(S_i^2S_j^2-2\langle S\rangle(S_iS_j^2+S_i^2S_j) +4S_iS_j\langle S\rangle^2). \tag{45}$$

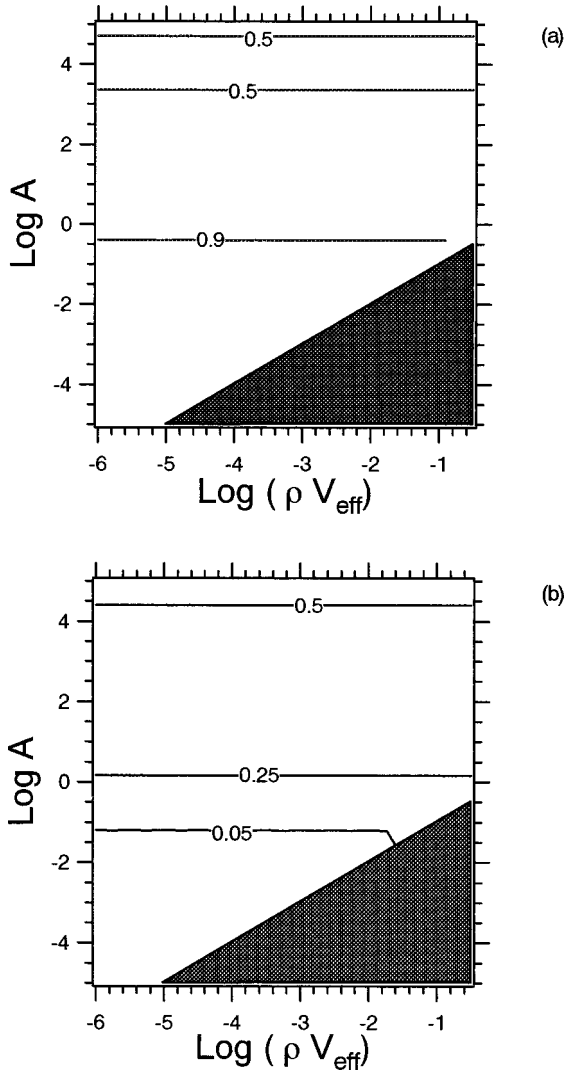

FIG. 3. Contours for the percentage error in the energy as calculated from the TPM as obtained via the unbiased (a) and biased (b) algorithms relative to the van Roij energy as a function of A and ρV_{eff}.

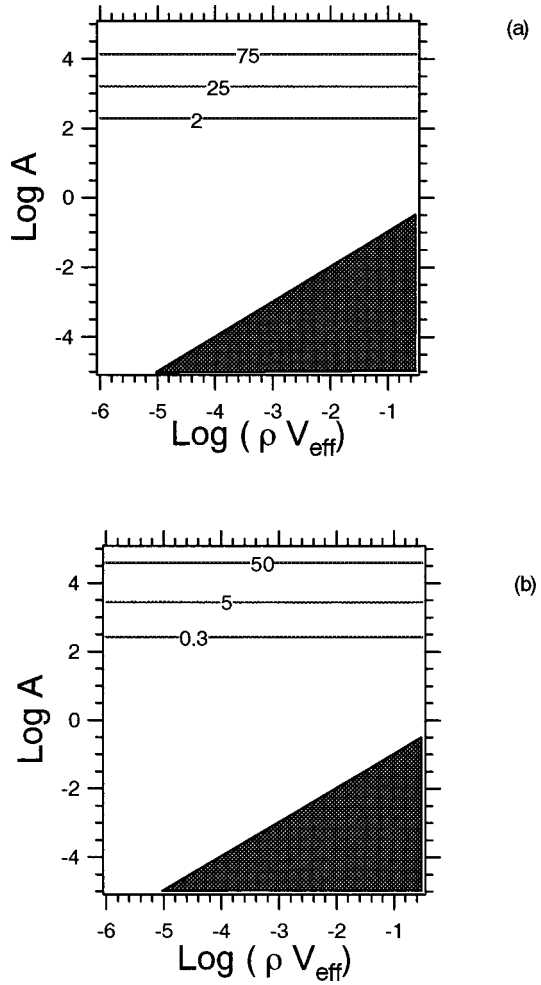

FIG. 4. Contours for the percentage error in the heat capacity as calculated from the TPM as obtained via the unbiased (a) and biased (b) algorithms relative to the van Roij energy as a function of A and ρV_{eff}.

VI. RESULTS OF TPM MODELING

Our aim in performing the TPM modeling is to provide a guide by which we can know when a biasing algorithm is needed to yield a result of a given precision using a simulation of reasonable length. The CPU overhead associated with the biased algorithm will not always be offset by the improved convergence rates of the simulation averages; also, implementing a biasing algorithm can be costly in terms of programming effort. It can therefore be very helpful to know beforehand if this expense is worthwhile.

We have observed a finite-size effect in our calculations that should be discussed before presenting the main results. The TPM analysis requires specification of a system size, given in terms of the maximum bond number S; the simulation being modeled by the TPM then would have a particle number N equal to $S+1$. A typical simulation has $N=108$, and this is the value we used for most of our TPM calculations. In contrast, the van Roij solution and the kinetic modeling are both performed for a system in which S/N takes on a continuum of values between zero and unity, implying an infinite system. The steady-state kinetic bond number agrees with the van Roij equilibrium bond number, and the rate constants used in the kinetic model are consistent with the transition probabilities that form the TPM. Hence one should expect that the energies obtained from the TPM method will agree with those from the van Roij solution. That they do agree is demonstrated in Fig. 3, which plots the percent error in the energy from the unbiased (a) and biased (b) TPM analyses relative to the results of van Roij (and, equivalently, the kinetic model). Note that the darkened area in these and all subsequent plots are areas where $\epsilon<0$, that describes a repulsive well. Since these states are not of interest to this study, we have excluded them from the plots. Both figures show that for all states (even those that violate the assumption of small ρV_{eff}) the difference between the van Roij and TPM energies is less than 1%.

Examination of the heat capacities obtained from the TPM and van Roij calculations through Fig. 4 show that at large A the disagreement with van Roij is great for both the biased and unbiased TPM algorithms. In these highly bonded states, we observed from the previous figure, however, that the energies from the TPM solution are described well relative to the van Roij results. Thus it seems that the probability distribution of states from the TPM solution is sufficient to

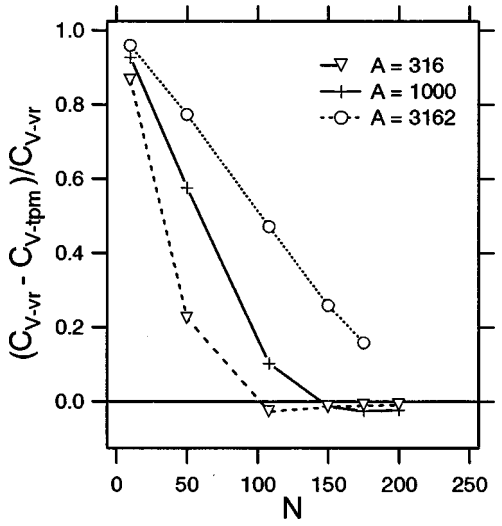

FIG. 5. The fractional error in the heat capacity from the TPM of the unbiased algorithm relative to the van Roij heat capacity as a function of system size. For the states with a large A, a larger N is needed to reduce the finite size effect inherent in the TPM method.

provide energies correctly but the fluctuations are poorly characterized. Such large A produces configurations dominated by a single long chain, sometimes present with several shorter ones. To validate that the discrepancy is indeed a finite-size effect, we looked at the fractional error in the TPM predicted heat capacity for the unbiased algorithm at large A states as a function of system size N. It is clear from Fig. 5 that as A increases finite-size effects grow, and a larger N is required to obtain a correct result. This is not a flaw of the TPM model *per se*, but is a ''feature'' of the Monte Carlo simulation that we are modeling. For this simple molecular model, the large A finite-size effects do not cause problems with the first-derivative quantities such as the energy, but manifest themselves in the second-derivative quantities such as the heat capacity.

The scaled fractional variance in the energy, given as $M\sigma_S^2/\langle S\rangle^2$ and referred to henceforth simply as the variance, is presented for each algorithm in Fig. 6. For the unbiased algorithm, the large variance at small ρV_{eff} implies that it is difficult to find bonding configurations *reliably* at this state, which is expected. The decrease in variance at large A for fixed ρV_{eff} is unexpected. One would expect a marked difficulty in reliably sampling the important configurations at large A through the unbiased algorithm, and this should result in an increased variance in the energy. The foregoing discussion has shown that substantial finite-size effects arise at about the point where the contours of Fig. 6(a) begin to bend back with increasing A. The finite-size effects are manifested in the bond fluctuations, which are the essential quantity examined in Fig. 6. Again, this is a property of the simulation of a small system, and is not something that arises because of some approximation in the TPM model. We would expect a simulation of an infinite system (and the TPM model of it) to show variance contours that continue up and to the right in Fig. 6(a). The biased algorithm shows the same large A feature as the unbiased algorithm, namely a small variance at large A. However, for the biased algorithm,

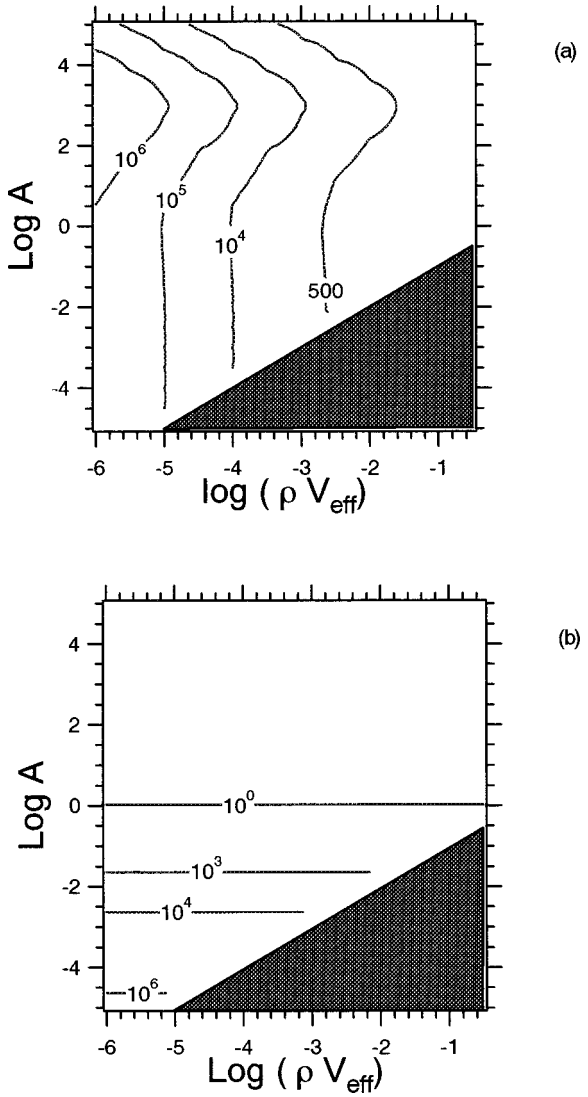

FIG. 6. Contours for the scaled fractional variance in the energy from the TPM as obtained via the unbiased algorithm (a) and the biased algorithm (b) relative to the TPM predicted energy.

no ρV_{eff} dependence is found for the variance. The variance increases as A decreases because it is presented on a percent basis in Fig. 6; at small A the variance is being divided by the square of the energy, which is very close to zero here. As expected, for almost all states the biased algorithm yields a smaller variance in the energy than the unbiased algorithm,

Before continuing, it should be emphasized that the asymptotic form for the scaled variance, which states that $M\sigma_S^2/\langle S\rangle^2$ is independent of M, is valid only for sufficiently large M. What constitutes ''sufficiently large'' depends on the thermodynamic state. It is reasonable to expect that the convergence of this group to its asymptotic form, indicating no memory of the initial state, would correspond to the rate at which the simulation averages converge to their equilibrium values. The latter value can be obtained from the kinetic model. At large A and small ρV_{eff} [and thus large $\exp(\beta\epsilon)$] the variances in Fig. 6 become meaningful only if one applies them to a sufficiently long simulation.

To use the figures provided in Fig. 6, one would determine what an acceptable error is for a study at a particular

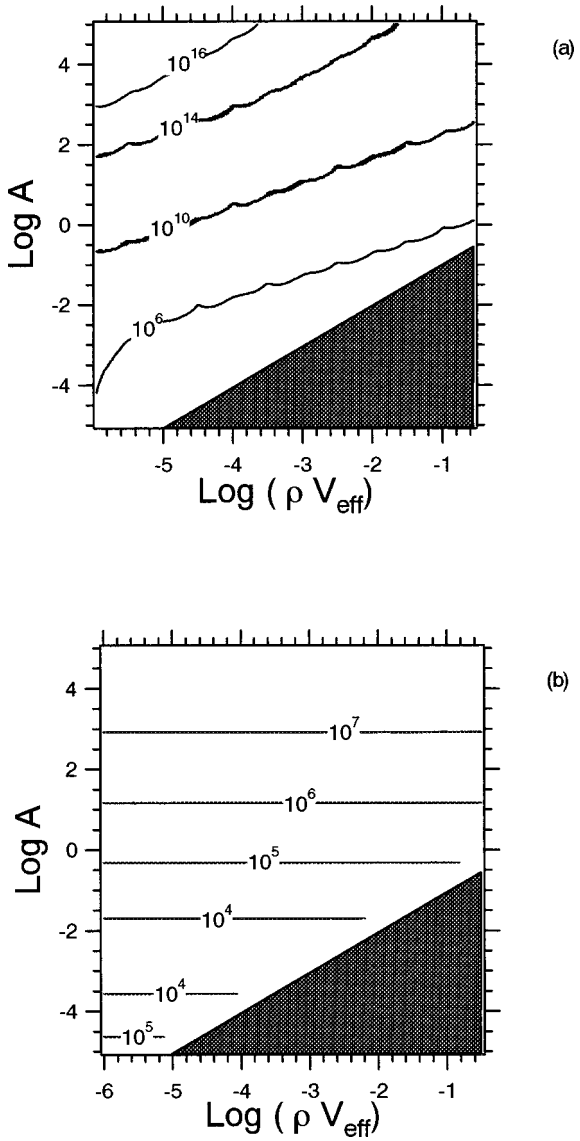

FIG. 7. Contours for the scaled fractional variance in the heat capacity from the TPM as obtained via the unbiased algorithm (a) and the biased algorithm (b) relative to the TPM predicted energy.

state. The density and temperature, along with order-of-magnitude estimates of V_{eff} and ϵ from the potential model, determine A and ρV_{eff}. For this state, one would determine the scaled fractional variance from Fig. 6(a) and calculate the value of M required to deliver the desired error. Then one would calculate from the kinetic model the length τ of a simulation required to achieve equilibrium. If τ is much smaller than M, then $M\sigma_S^2/\langle S\rangle^2$ is likely to be in the asymptotic regime where it is independent of M, and the variance calculation can be judged as valid. At this point, one must assess whether M describes a simulation of reasonable length. If not, a biasing algorithm should be considered to bring M to a more manageable range.

The improved accuracy delivered by the biased algorithm relative to the unbiased algorithm is highlighted in the scaled variances of the heat capacity. This information is provided in Fig. 7. At the most difficult state to simulate, large A and small ρV_{eff}, the biased algorithm exhibits an improvement of about ten orders of magnitude in the precision with which the heat capacity can be measured. At the states where bonding is less prevalent, specifically small A, the utility of a biasing approach is greatly diminished.

VII. CONCLUDING REMARKS

The ideal association model on which this work is based has proved very useful in conducting our studies of the behavior of simulations of associating systems. The model yields to various types of analysis, and leaves no ambiguity about what constitutes an association bond. It is of course a very unrealistic model of an associating system. Real system exhibit repulsion and various forms of attraction, and these features may dominate the behavior in a way that renders the present analysis irrelevant. The results presented here gain validity as the association becomes strong compared to these other parts of the potential. Even if the comparison is equivocal, as a qualitative guide the results presented here should be helpful in gauging where a simulation of a given system might encounter difficulty.

ACKNOWLEDGMENTS

Acknowledgment is made to the Donors of the Petroleum Research Fund, administered by the American Chemical Society, for partial support of this research. This work is made possible also by funding from the National Science Foundation. D.P.V.J. would like to thank Sandeep Pandit for helpful discussions on this work.

[1] P. W. Atkins, *Physical Chemistry* (W. H. Freeman, New York, 1994).
[2] J. de Pablo, J. Prausnitz, H. Strauch, and P. Cummings, J. Chem. Phys. **93**, 7355 (1990).
[3] M. E. Cournoyer and W. L. Jorgensen, Mol. Phys. **51**, 119 (1984).
[4] M. van Leeuwen and B. Smit, Phys. Rev. Lett. **71**, 3991 (1993).
[5] P. Jedlovszky and R. Vallauri, Mol. Phys. **92**, 331 (1997).
[6] N. A. Busch, M. S. Wertheim, Y. C. Chiew, and M. L. Yarmush, J. Chem. Phys. **101**, 3147 (1994).
[7] D. M. Tsangaris and J. J. dePablo, J. Chem. Phys. **101**, 1477 (1994).
[8] F. Bresme, E. Lomb, and J. L. F. Abascal, J. Chem. Phys. **106**, 1569 (1997).
[9] D. Ghonasgi, V. Perez, and W. Chapman, J. Chem. Phys. **101**, 6880 (1994).
[10] D. Ghonasgi and W. G. Chapman, Mol. Phys. **80**, 161 (1993).
[11] D. Ghonasgi and W. G. Chapman, Mol. Phys. **79**, 291 (1993).
[12] W. G. Chapman, K. E. Gubbins, C. G. Joslin, and C. G. Gray, Fluid Phase Equilibria **29**, 337 (1986).
[13] J. K. Johnson and K. E. Gubbins, Mol. Phys. **77**, 1033 (1992).
[14] D. Ghonasgi and W. G. Chapman, Mol. Phys. **83**, 145 (1994).
[15] E. Muller, L. Vega, and K. Gubbins, Int. J. Thermophys. **16**, 705 (1995).
[16] W. G. Chapman, K. Gubbins, G. Jackson, and M. Radosz, Fluid Phase Equilibria **52**, 31 (1989).
[17] J. I. Siepmann and D. Frenkel, Mol. Phys. **75**, 59 (1992).
[18] N. A. Busch, M. S. Wertheim, and M. L. Yarmush, J. Chem. Phys. **104**, 3962 (1996).
[19] R. van Roij, ''Simple theories of complex fluids,'' Thesis, FOM—Institute for Atomic and Molecular Physics (1996).
[20] R. van Roij, Phys. Rev. Lett. **76**, 3348 (1996).
[21] R. A. Heidemann and J. M. Prausnitz, Proc. Natl. Acad. Sci. USA **73**, 1773 (1976).
[22] D. Visco, Jr. and D. Kofke, J. Chem. Phys. **109**, 4015 (1998).
[23] D. L. Isaacson and R. W. Madsen, *Markov Chains* (Wiley, New York, 1976).
[24] R. A. Howard, *Dynamics Probabilistic Systems, Vol. 1, Markov Models* (Wiley, New York, 1971).
[25] D. A. Kofke and P. T. Cummings, Mol. Phys. **92**, 973 (1997).